American Journal of Biodiversity
https://biojournals.us/index.php/AJB
ISSN: 2997-3600

Design and Implementation Oxygen Sensor Used Graphene Metal Nanocomposites by LIFT Method

Ala'a Hameed Kadom
University: Al-Isra University / Technical College / Department of Medical Devices Engineering Technology

Ahmed Sameer Hachim, Tiba Laiq Neamah
Al-Farahidi University Medical DEVICES ENGINEERING

Hadeel Qasim Sattar
Middle Technical University Medical Devices Engineering

Waleed Sabah Mahdi
Bilad Alrafidain University Engineer Medical Devices

Received: 2024, 15, Dec
Accepted: 2025, 21, Jan
Published: 2025, 04, Feb

Annotation: Nanoparticles aroused great interest. In this study, a gas sensor (oxygen sensor) was fabricated using Laser-induced forward transferuses with nanomaterials (grapheneGO - nanosilver Ag- titanium dioxideTiO2) Where the nanomaterials were diagnosed using a (Filed Emission scanning electron microscopy FE-SEM) and the materials were within the nanoscale, the sensor was used to measure the gases in the room, as well as the leakage of gases in the gas systems and others.

Keywords: nanosilver, grapheneGO, titanium, dioxideTiO2.

Introduction

Laser material processing has become an essential manufacturing technique in thin – film technology. Around 1439 Johannes Gutenberg developed the first movable type printing press in Europe .the invention represented such a boost in the productivity of written works. Laser – induced forward transfer (LIFT) constitutes an additional contribution to the large set of direct writing techniques. The primary advantages of this technique are low cost, environmental friendliness and fast turnaround from concept to prototype [1].Spin coating is a commercial and low-cost technique for the fabrication of large-area coatings and thin films, but it is a stochastic process that is hard to control, as far as the fabrication of thin coatings and solid films is concerned. On the other hand, drop-casting is a facile and more controllable coating technique but its application is limited to small-area thin solid films and coatings [2]. As such, green synthesis is regarded as an important tool to reduce the destructive effects associated with the traditional methods of synthesis for nanoparticles commonly utilized in laboratory and industry (using natural extracts) [3]. Polymers are an important class of materials having different applications in various fields of science and technology, particularly in optics, electronics, biotechnology, photonics and space research. Optical properties of PMMA taking place during the irradiation particularly the absorption of moisture and the condition for dimerization of carbonyl groups in PMMA.

1. 2 Literature Survey

Chem. Chem. Phys.(2013) Graphene is a single-atom thick, two-dimensional sheet of carbon that is characterized by exceptional chemical, electrical, material, optical, and physical properties. As a result, graphene and related materials, such as graphene oxide and reduced graphene oxide, have been brought to the forefront in the field of sensing. Recently, a number of reports have demonstrated that graphene–nanoparticle hybrid structures can act synergistically to offer a number of unique physicochemical properties that are desirable and advantageous for sensing applications. These graphene–nanoparticle hybrid structures are particularly interesting because not only do they display the individual properties of the nanoparticles and of graphene, but they can also exhibit additional synergistic properties thereby enhancing the achievable sensitivity and selectivity using a variety of sensing mechanisms. As such, in this perspective, we will discuss the progress that has been made in the development and application of graphene–nanoparticle hybrid sensors and their future prospects. In particular, we will focus on the preparation of graphene–nanoparticle hybrid structures as well as their application in electronic, electrochemical, and optical sensors.[4]

Chau Hai Thai Vu&Joon Seok Lee (2015) We first report on the synthesis of graphene oxide-wrapped TiO_2 nanoparticles (GO-TiO_2 NPs) as a self-adhesive photocatalyst for UV-activated colorimetric oxygen detection. Methylene blue (MB), a redox dye for colorimetric oxygen indication, strongly adsorbed onto GOTiO_2 NPs by both electrostatic and π–π stacking interactions. The chemical attraction between GO and MB significantly decreased dye leakage, which is a serious problem of colorimetric oxygen indicators; MB leaching from GO-TiO_2based film was fivefold lower than that from conventional TiO_2-based film. This novel MB/GO-TiO_2/glycerol/hydroxyethyl cellulose film was successfully bleached by UV irradiation, and it regained its blue color rapidly in the presence of oxygen, demonstrating its useful functionality as a UV-activated colorimetric oxygen indicator.

M. T. Aunkor et al. (2016) this paper focused on reduced the harmful of chemical agents that effect on human and environment. They reduced the oxygen groups using different friendly environmentally substance.[5]

Emel Önal, Zeynep Ay 2016 Room temperature phosphorescent oxygen sensors have been designed by embedding symmetric palladium(II) or platinum(II) mesotetraphenylporphyrins in poly(1-trimethylsilyl-1-propyne) in the form of nanofibers along with/without silver nanoparticles. These materials combine the advantages of the high oxygen sensitivity of porphyrins and the enhanced surface area of porous nanofibers. Phenylacetylide bearing palladium(II) or platinum(II) *meso*tetraphenylporphyrins (Pd-TPA, Pt-TPA, Pd-TPP and Pt-TPP) were designed to enhance phosphorescence quantum yields as well as sensitivity towards oxygen. Their syntheses were achieved by 2 alternative methods including successive metallation reactions and Sonogashira coupling *via* optimization of the synthetic strategies and conditions. The respective effect of the metal (Pd or Pt) and substituent on phosphorescence quantum yield as well as other photophysical properties was considered. The sensing performances of the corresponding silverfree and silver doped nanofibers were tested in the oxygen concentration range of 0.0–100.0%. The offered composites provided the advantages of fast response, enhanced sensitivity, reversible and long lasting response, higher Stern–Volmer constants (K_{SV}) and low limit of detection values extending to 7.5 ppm for oxygen.

K.K.H. De Silva et al. (2017) explained the various methods of synthesis of graphene oxide GO like use Hummer ' and Tour methods. And the synthesis of reduced graphene oxide using different chemical reduction (hydrogen sulphide, hydrazine, alkaline solution, sodium citrate, plant extract, amino acid and microorganism) and they described the optical and electrical properties. The characterized of properties by XRD, FTIR and AFM, in XRD the location of the peaks at ($2\theta = 11^{\circ}$, $25)^{\circ}$ degree of graphene oxide and reduced sequentially. The FTIR shows the reduced of oxygen. [6]

Melvin Jia – Young Tia et al. (2018) studied graphene oxide and reduced graphene oxide at low coast and environment friendly synthesis using green tea extract. And characterized by FTIR, XRD, UV- Vis, EDX, SEM. FTIR provide the reduction of oxygen and UV- Vis spectra showed absorption peaks at 230nm for GO and 280 nm for rGO. SEM showed wrinkled and flaky structure for both GO and rGO while the EDX showed the composition of them.[7]

Pol Sopeña et al. (2018) they used Laser-induced forward transfer (LIFT) with different pulse laser power in Ag ink to deposited it in substrate. Through the action of a laser pulse focused on a liquid film, usually called donor film, the laser-induced forward transfer (LIFT) technique allows transferring liquids from that film to a receiver substrate. The laser pulse is absorbed in the donor film, which leads to the generation of a bubble at the interface between the transparent donor substrate and the ink. The further expansion of the bubble results in the formation of a jet that propagates forward until it impacts the receiver substrate, and thus prompts the formation of a sessile droplet. Thickness decreases with increasing laser power for a given scan speed and, in general, increases with scan speed for the same power.[8]

Teppei Araki et al (2018) laser-induced forward transfer used for non-contacted printing techniques, Silver nanowires (AgNWs) used as wearable devices due to their high flexibility and high conductivity. A patterned transparent electrode showed over 80% in optical transmittance and less than 100 Ω sq^{-1} in sheet resistance by the optimized LIFT technique.[9]

Huan Wang et al (2019) synthesized and characterized Uniform silver nanowires (AgNWs) to fabricate high-performance transparent conductive films (TCFs) through spin-coating at a variable speed. In XRD the crystal lattice fringes of one part of an individual nanowire with a spacing distance of ~2.05 and 2.36 Å, corresponding to (002) and (111) planes of FCC silver nanostructures, respectively. One series of diffraction spots can be indexed as (111), (002), (200), (220) and (311) planes. The peaks at 423, 350 and 380 nm could be attributed to the nanoparticles. [10]

Matthew Praeger et al (2020) used LIFT technique, Under optimal laser exposure conditions, and in a low-pressure gas environment, circular regions of graphene with approximately 30 µm diameter were successfully transferred from the donor to the receiver substrate. That confirmed by optical and electron microscopy. SEM imaging reveals that the graphene fragments sometimes lie flat on the receiving substrate and sometimes curl up.[11]

Kevin Varghese Alex 2020 In this work, sensing and photocatalytic activities of green synthesized silver nanoparticles (Ag NPs) are investigated. Ag NPs have been synthesized by the reduction of silver nitrate ($AgNO_3$) using different leaf extracts. An optimum surface plasmon resonance (SPR) behavior is obtained for neem leaf extracts because of the presence of a high concentration of diterpenoids, as evidenced from gas chromatography mass spectroscopy results. The underlying mechanism for the formation of Ag NPs is highlighted. The Ag NPs are in spherical shape and exhibit the hexagonal crystal phase and also show a good stability. The biosensing property of the Ag NPs is evaluated using mancozeb (MCZ) agrofungicide, and the SPR peak position exhibited a linear response with MCZ concentration. The sensitivity is found to be 39.1 nm/mM. Further, the photocatalytic activity of Ag NPs is tested using 0.5 mM MCZ solution as a model under UV–visible illumination. It is observed that photocatalytic activity is caused by the formation of reactive oxygen species. Therefore, the green synthesized Ag NPs are potential candidates for biosensing and photocatalytic applications.

Xinwei Wang at el (2021) they achieved excellent quality printing of graphene oxide by used Laser Induced Forward Transfer (LIFT). Droplet printing using LIFT method with the modified donor substrate and various pulse energies was investigated. The droplet diameter grew linearly from 40 to 165 μm with the increasing pulse energy from 4 to 11μJ.[12]

1.3 Aims of work

- ✓ Preparation thin films as oxygen sensor using graphene Nano sheet (GO) with titanium dioxide (TiO2) by LIFT method.
- ✓ Characterized used scanning electron microscopy (SEM) and EDX.
- ✓ Applied the prepared films used oxygen champers.

LIFT Method

Laser-induced forward transferuses laser pulses of sufficient intensity aimed through a transparent substrate coated with a thin layer of material to achieve discrete (or digital) material transfer in the forward laser direction. [13] The transferred material can be collected on a separate substrate facing the thin layer. The straightfor wardness of this approach led to many groups to try it with different types of materials and, despite its inherent simplicity, LIFT exists in many different variations.LIFT is compatible with virtually any type of material, and takes place under ambient atmospheric conditions, thus making it one of the most versatile digital microfabrication techniques developed to date. The LIFT techniques are a perfect example of additive LDW, capable of generating high-resolution patterns without the need for lithographic steps afterwards. In fact, the same equipment setup required by LIFT can be used for other LDW processes such as subtractive (laser micromachining), and modifying (laser sintering, laser annealing, etc.) . What makes LIFT unique is its ability to laser transfer such a wide variety of materials with relatively high resolution conformal to the surface. For example, the LIFT process does not have a deleterious effect on the electrical, chemical, and even biological properties of the voxels of material forming the digital pattern. The ability to laser transfer functional materials and then process them or modify them in order to achieve the required properties and behavior is unique and represents one of the major advantages of laser-based microfabrication techniques. LIFT was introduced by Bohandy in 1986 . In this technology, the deposition material is pre-coated, with a thickness of less than a few hundreds of nanometers, on one side of a transparent support called target or donor.The substrate, or the receptor, is mounted in a very small standoff distance (25–75 μm) from the donor, while the thin film faces the substrate. The transparent support is radiated by the focused beam of a pulsed laser from the back. The laser energy is absorbed by the pre-coated material, and the generated heat ablates the film from the support.The separated film is transferred to the substrate, where it is deposited.Typical laser pulse durations for the ablation and transfer process are in the range of nanoseconds to femtoseconds . Patterning can be performed by moving the laser beam relative to the substrate. The thickness of the deposited patterns is controlled by the repetition of the laser radiation process.The LIFT process has been incorporated for the deposition of various metals, oxides, polymers, semiconductors, and biological materials. Dielectric inks (Au , Sn, Ni) InOx active optical structures have been deposited with LIFT.LIFT has also been utilized for the deposition of Al thin films using a femtosecond laser , surface patterning with Au , and semiconductor die transfer . Nanocrystal quantum dot emitters have been deposited by LIFT.For this application, CdSe(CdS) was spincasted on the donor support with pre-deposited layers of triazene polymer and aluminum. A UV laser with a wavelength of 193 nm was used for the exposure .A modified LIFT process has also been introduced for sub-micron parallel depositions. In the modified method, the incident laser beam is focused through self-assembled micro-sphere arrays placed on the back side of a quartz wafer. On the other side, the deposition material is pre-coated.LIFT is a pyrolytic process and cannot be used for the deposition of materials with crystallization temperature above room temperature. In addition, it has some disadvantages in terms of uniformity, morphology, adhesion of the coatings to the substrate, deposition line width, impurities of coatings, ablation of the support, and material implantation into the substrate which have been overcome in matrix-assisted pulsed laser evaporation direct write (MAPLE DW) method.

Results and Discussion

sensor for room oxygen temperature gas sensing

graphene oxide is prevailing over the diferent derivatives of graphene due to its remarkable characteristics such as excellent response characteristics; chemical stability, large specifc surface area, high carrier mobility, and good mechanical strength. All of these features of rGO makes it an ideal candidate for gas detection[65] . Moreover, in the modern era, the focus of the researcher is oriented towards fexible gas sensor having good sensing ability at room temperature (RT). Tis fexible sensor (i.e. electronic skin) can be attached to the human body for detecting and sensing the pollutant gases[66] . Tere are various fexible materials that can be utilized as membrane formation. Polyvinylidene fuoride (PVDF) is a piezoelectric material having good UV and thermal stability, good mechanical strength, excellent chemical resistance and membrane formation features. It also has potential applications towards energy conversion such as energy harvesters and micro electrical-mechanical devices[67-68] . Hence, the above literature survey motivates to develop a fexible and high sensitive H2 gas sensor. By considering all the aspects, a tertiary nanocomposite based fexible hydrogen gas sensor has been fabricated by using rGO, SnO2, and PVDF to operate at room temperature. It is interesting to note that there is/are no report/s on rGO/SnO2/PVDF nanocomposites as a H2 gas sensor. Hence, the 1st time such a sensor is reported for the H2 gas sensing applications. Te interdigitated electrode of Cr metal has been deposited by using E-beam evaporation system. Various characterization tools have been used to determine the diferent properties of the thick flm. Te sensor has been tested inside a controlled gas chamber with I~V source meter for diferent gases and for different gas concentration at room temperature. It is observed that the proposed sensor is easy to prepare (low cost) and fexible (polymer) in nature and, exhibits excellent H2 gas sensing at room temperature. Hence, the present study opens a new window for accomplishing a polymer based tertiary nanocomposite H2 gas sensor.

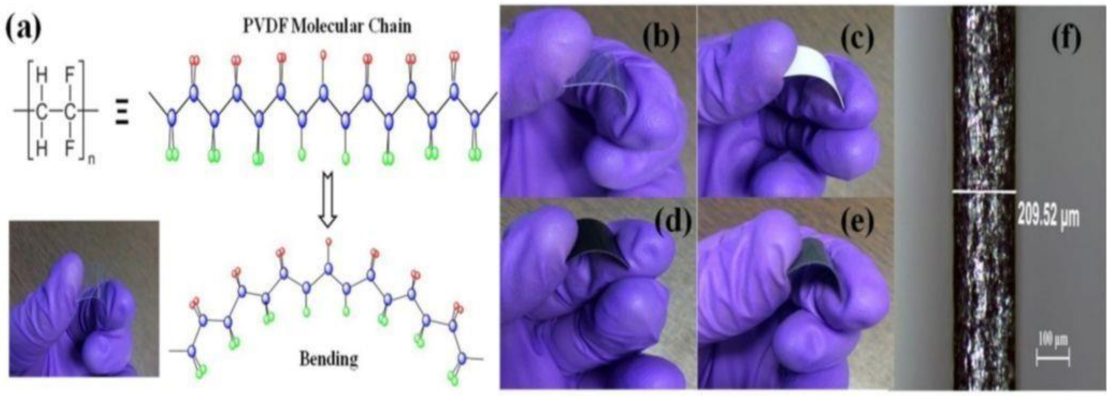

Fig 2.11 (A) Schematic illustration of PVDF molecular chain, Photographs of (B) PVDF, (C) SnO_2, (D) rGO/ PVDF, (E) rGO/SnO_2/PVDF at bending position, and (F) transverse optical microscope image of rGO/SnO_2/ PVDF thick films (thickness ~209.52 μm).

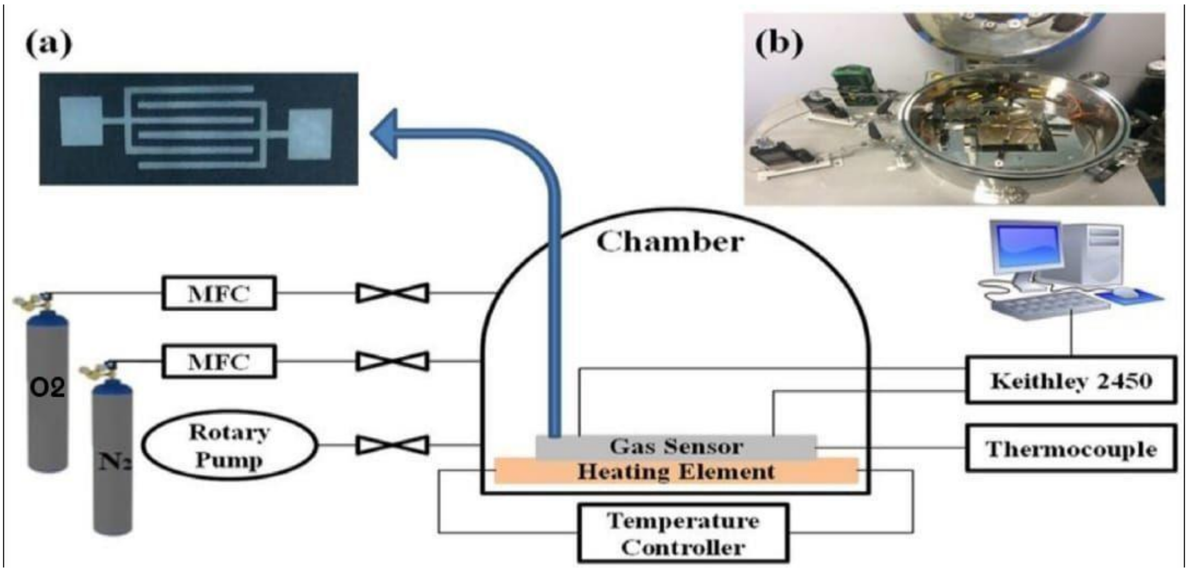

Fig 2.12 Schematic diagram of the gas chamber for sensing of gas in a controlled environment with (inset) (A) optical image of the fabricated sensor and (B) Real image of the gas chamber measurement system.

Gas Sensing Analysis

The adsorption mechanism in the above mentioned sensor is based on physisorption and chemisorption process. In the physisorption process, hydrogen atoms adsorbed on the surface of PVDF nanomaterial by van der Waals forces[69–71]. These van der Waals forces are weak in nature, which leads to a small variation in conductance for PVDF nanomaterial sensing layer. Whereas in the chemisorption process, due to the formation of covalent bond, it has strong van der Waals forces[72,73]. This chemisorption mechanism has been seen for rGO and SnO_2 nano-composite with PVDF nanomaterial. When these nanocomposite based sensor is exposed to air, oxygen species adsorbed on material surface by occupying the electrons from conduction band to make anions of chemisorbed oxygen (O_2 −(ads)). It further results in the formation of space charge region, i.e. depletion region[74]. figure 11 shows the sensor response (%) of PVDF, rGO/PVDF, SnO_2/PVDF and rGO/SnO_2/PVDF nanocomposites for different gas concentrations at room temperature. The gas response of the sensor has been tested for different concentrations (i.e. 10 PPM, 50 PPM, 100 PPM, 200 PPM, 500 PPM, and 1000 PPM) of H_2 gas for above mentioned films. It has been observed that the gas concentration has a great impact on the sensor response where the response and recovery time is calculated as the time taken to reach 90% of its equilibrium value[75]. The chemisorption process takes more time than the physisorption process because of high energy requirement for the formation of covalent bonds[74]. This effect also has been observed for the present sample specimens.

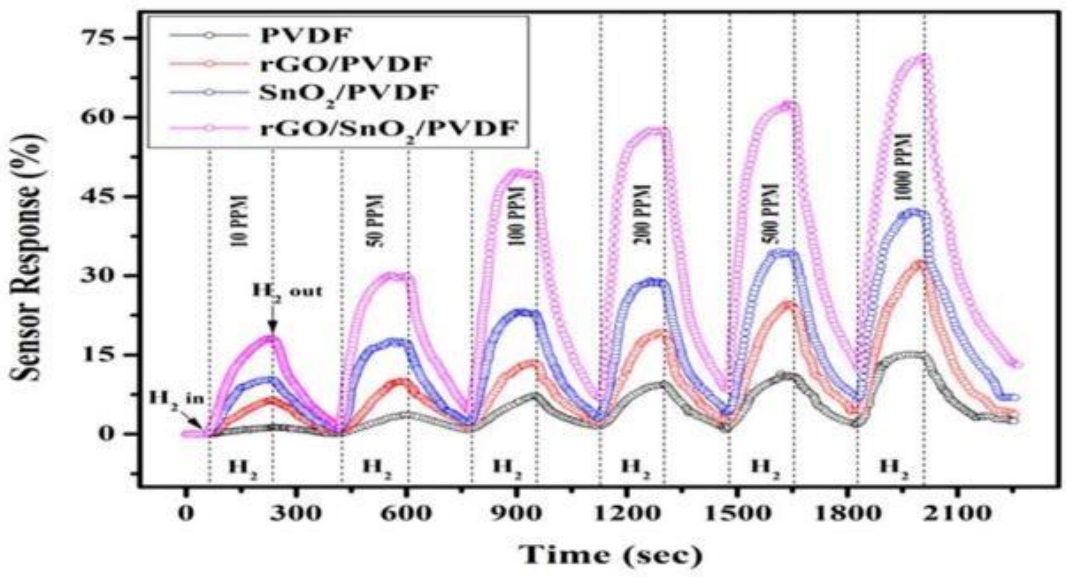

Fig 2.11 Sensor response of PVDF, rGO/PVDF, SnO2/PVDF, and rGO/SnO2/PVDF gas sensor for diferent H2 gas concentrations.

2.8 Gas detector

is the process of identifying potentially hazardous gas leaks by sensors. Additionally a visual identification can be done using a thermal camera These sensors usually employ an audible alarm to alert people when a dangerous gas has been detected. Exposure to toxic gases can also occur in operations such as painting, fumigation, fuel filling, construction, excavation of contaminated soils, landfill operations, entering confined spaces, etc.

Types

Gas detectors can be classified according to the operation mechanism

(semiconductors,[76] oxidation, catalytic, photoionization, infrared, etc.). Gas detectors come packaged into two main form factors: portable devices and fixed gas detectors.Portable detectors are used to monitor the atmosphere around personnel and are either hand-held or worn on clothing or on a belt/harness. These gas detectors are usually battery operated. They transmit warnings via audible and visible signals, such as alarms and flashing lights, when dangerous levels of gas vapors are detected.Fixed type gas detectors may be used for detection of one or more gas types. Fixed type detectors are generally mounted near the process area of a plant or control room, or an area to be protected, such as a residential bedroom. Generally, industrial sensors are installed on fixed type mild steel structures and a cable connects the detectors to a SCADA system for continuous monitoring. A tripping interlock can be activated for an emergency situation.

Electrochemical

Electrochemical gas detectors work by allowing gases to diffuse through a porous membrane to an electrode where it is either chemically oxidized or reduced. The amount of current produced is determined by how much of the gas is oxidized at the electrode, indicating the concentration of the gas. Manufactures can customize electrochemical gas detectors by changing the porous barrier to allow for the detection of a certain gas concentration range[77]. Also, since the diffusion barrier is a physical/mechanical barrier, the detector tended to be more stable and reliable over the sensor's duration and thus required less maintenance than other early detector technologies.However, the sensors are subject to corrosive elements or chemical contamination and may last only 1–2 years before a replacement is required. Electrochemical gas detectors are used in a wide variety of environments such as refineries, gas turbines, chemical plants, underground gas storage facilities, and more.[78]

Catalytic bead (pellistor)

Catalytic bead sensors are commonly used to measure combustible gases that present an explosion hazard when concentrations are between the lower explosion limit (LEL) and upper explosion limit (UEL). Active and reference beads containing platinum wire coils are situated on opposite arms of a Wheatstone bridge circuit and electrically heated, up to a few hundred degrees C. The active bead contains a catalyst that allows combustible compounds to oxidize, thereby heating the bead even further and changing its electrical resistance. The resulting voltage difference between the active and passive beads is proportional to the concentration of all combustible gases and vapors present. The sampled gas enters the sensor through a sintered metal frit, which provides a barrier to prevent an explosion when the instrument is carried into an atmosphere containing combustible gases. Pellistors measure essentially all combustible gases, but they are more sensitive to smaller molecules that diffuse through the sinter more quickly. The measureable concentration ranges are typically from a few hundred ppm to a few volume percent. Such sensors are inexpensive and robust, but require a minimum of a few percent oxygen in the atmosphere to be tested and they can be poisoned or inhibited by compounds such as silicones, mineral acids, chlorinated organic compounds, and sulfur compounds.

Photoionization

Photoionization detectors (PIDs) use a high-photon-energy UV lamp to ionize chemicals in the sampled gas. If the compound has an ionization energy below that of the lamp photons, an electron will be ejected, and the resulting current is proportional to the concentration of the compound. Common lamp photon energies include 10.0 eV, 10.6 eV and 11.7 eV; the standard 10.6 eV lamp lasts for years, while the 11.7 eV lamp typically last only a few months and is used only when no other option is available. A broad range of compounds can be detected at levels ranging from a few ppb to several thousand ppm. Detectable compound classes in order of decreasing sensitivity include: aromatics and alkyl iodides; olefins, sulfur compounds, amines, ketones, ethers, alkyl bromides and silicate esters; organic esters, alcohols, aldehydes and alkanes; H_2S, NH_3, PH_3 and organic acids. There is no response to standard components of air or to mineral acids. Major advantages of PIDs are their excellent sensitivity and simplicity of use; the main limitation is that measurements are not compound-specific. Recently PIDs with pre-filter tubes have been introduced that enhance the specificity for such compounds as benzene or butadiene. Fixed, hand-held and miniature clothing-clipped PIDs are widely used for industrial hygiene, hazmat, and environmental monitoring.

Infrared point

Infrared (IR) point sensors use radiation passing through a known volume of gas; energy from the sensor beam is absorbed at certain wavelengths, depending on the properties of the specific gas. For example, carbon monoxide absorbs wavelengths of about 4.2-4.5 μm[79]. The energy in this wavelength is compared to a wavelength outside of the absorption range; the difference in energy between these two wavelengths is proportional to the concentration of gas present. This type of sensor is advantageous because it does not have to be placed into the gas to detect it and can be used for remote sensing. Infrared point sensors can be used to detect hydrocarbons and other infrared active gases such as water vapor and carbon dioxide. IR sensors are commonly found in waste-water treatment facilities, refineries, gas turbines, chemical plants, and other facilities where flammable gases are present and the possibility of an explosion exists[80]. The remote sensing capability allows large volumes of space to be monitored.Engine emissions are another area where IR sensors are being researched. The sensor would detect high levels of carbon monoxide or other abnormal gases in vehicle exhaust and even be integrated with vehicle electronic systems to notify drivers.

Infrared imaging

Infrared image sensors include active and passive systems. For active sensing, IR imaging sensors typically scan a laser across the field of view of a scene and look for backscattered light at the absorption line wavelength of a specific target gas. Passive IR imaging sensors measure spectral changes at each pixel in an image and look for specific spectral signatures that indicate the presence of target gases[81]. The types of compounds that can be imaged are the same as those that can be detected with infrared point detectors, but the images may be helpful in identifying the source of a gas.

Semiconductor

Semiconductor sensors, also known as metal-oxide-semiconductor sensors (MOS sensors) detect gases by a chemical reaction that takes place when the gas comes in direct contact with the sensor. Tin dioxide is the most common material used in semiconductor sensors, and the electrical resistance in the sensor is decreased when it comes in contact with the monitored gas[82]. The resistance of the tin dioxide is typically around 50 kΩ in air but can drop to around 3.5 kΩ in the presence of 1% methane[83]. This change in resistance is used to calculate the gas concentration. Semiconductor sensors are commonly used to detect hydrogen, oxygen, alcohol vapor, and harmful gases such as carbon monoxide[84]. One of the most common uses for semiconductor sensors is in carbon monoxide sensors. They are also used in breathalyzers. Because the sensor must come in contact with the gas to detect it, semiconductor sensors work over a smaller distance than infrared point or ultrasonic detectors.MOS sensors can detect different gases, such as carbon monoxide, sulfur dioxide, hydrogen sulfide, and ammonia. Since the 1990s, MOS sensors have become important environmental gas detectors. MOS sensors although very versatile, suffer from the problem of cross sensitivity with humidity. The cause for such behaviour has been attributed to interaction of hydroxyl ions with the oxide surface[85]. Attempts have been made to reduce such interference using algorithmic optimizations[86].

Ultrasonic

Ultrasonic gas leak detectors are not gas detectors per se. They detect the acoustic emission created when a pressured gas expands in a low pressure area through a small orifice (the leak). They use acoustic sensors to detect changes in the background noise of its environment. Since most high-pressure gas leaks generate sound in the ultrasonic range of 25 kHz to 10 MHz, the sensors are able to easily distinguish these frequencies from background acoustic noise which occurs in the audible range of 20 Hz to 20 kHz[87]. The ultrasonic gas leak detector then produces an alarm when there is an ultrasonic deviation from the normal condition of background noise. Ultrasonic gas leak detectors cannot measure gas concentration, but the device is able to determine the leak rate of an escaping gas because the ultrasonic sound level depends on the gas pressure and size of the leak. Ultrasonic gas detectors are mainly used for remote sensing in outdoor environments where weather conditions can easily dissipate escaping gas before allowing it to reach leak detectors that require contact with the gas to detect it and sound an alarm. These detectors are commonly found on offshore and onshore oil/gas platforms, gas compressor and metering stations, gas turbine power plants, and other facilities that house a lot of outdoor pipeline.

Holographic

Holographic gas sensors use light reflection to detect changes in a polymer film matrix containing a hologram. Since holograms reflect light at certain wavelengths, a change in their composition can generate a colorful reflection indicating the presence of a gas molecule[88]. However, holographic sensors require illumination sources such as white light or lasers, and an observer or CCD detector.

Laser Introduced Forward Transform (LIFT)

This method involved the following steps:

1-Drop casting method

Poly Methyl Methacrylate (PMMA) (1 wt. % solution from toluene) casting on glass using micro needle (length 75ml, diameter 0.5 mm) then from table (3-3) of liquid sample proportion of (GO +Ag+ TiO_2), it used to casting on (glass + PMMA) substrate.

Table (3-1) illustrates the proportion of liquid (toluene) samples.

Samples code	GO g/25ml	Ag or TiO_2 g/25ml
A	o.15	0.015
B	0.15	0.025
C	0.15	0.035
	50ml	

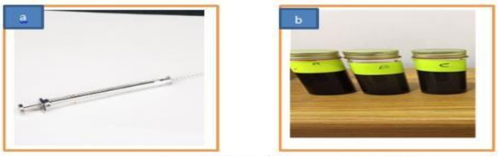

a. micro needle b. the proportion of liquid samples.

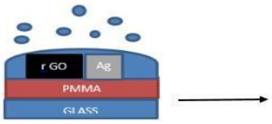

illustrates drop casting method.

Fig 3.1 Experimental work Part 1

Laser Introduced Forward Transform:-

laser (coherent Mira 900 Ti – sapphire oscillator with pulse amplifier) with energy 325 mJ/pulse, frequency 10 Hz, wavelength 1056nm, pulse duration 20ns and the laser spot 2.5 cm. The laser pulse will strike the (rGo + Ag OR TiO_2 +glass + PMMA) substrate (donor substrate) to transform the (rGo + Ag+ PMMA) to the accepter substrate.

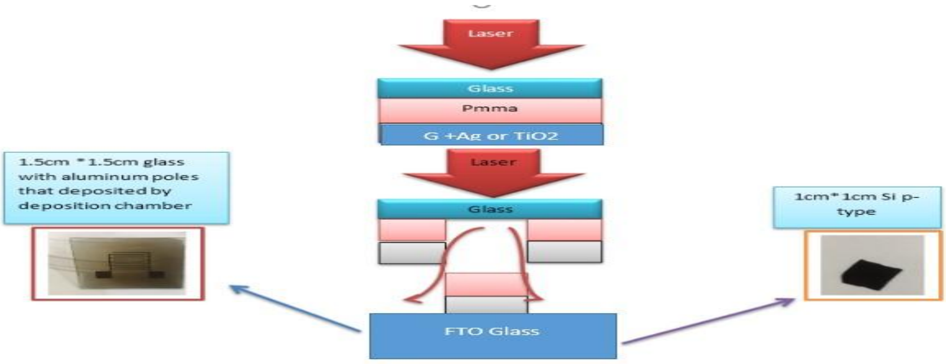

Fig 3.2 Experimental work Part 2

Filed Emission scanning electron microscopy FE-SEM

The topography of the films prepared was studied by scanning electron microscopy type (MIRA3 FEG-SEM) with different magnification powers. The resolution is 5 nm and the magnification ability is X10^6 with the voltage of 30 kv. It used to measure the surface roughness of samples and the grain size of PMMA/graphene /Ag nanoparticles/ titanium dioxide.

Gas chamber detector

Fig 3.3 laser LIFT method

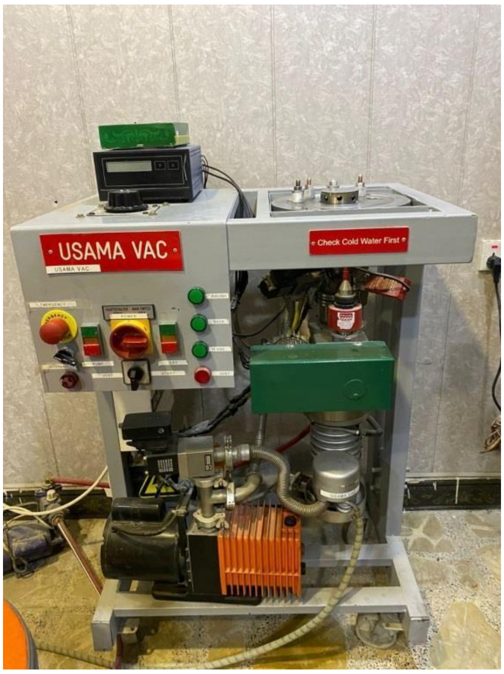

Fig 3.4 Gas chamber detector

4.1 Filed Emission scanning electron microscopy FE-SEM

In LIFT SEM images showed in figure (4-1), (4-2) and (4-3) (G : Ag) , (G :TiO_2) and (G : Ag: TiO_2) films, it was found AgNPs are deposited and prevail on Nano reduced graphene flakes, the average particles size of AgNPs is about ~25 nm. The AgNPs were deposited on G flakes due to the strong electrostatic and electronic interaction between G flakes and AgNPs while the titanium dioxide exhibit spherical aggregation of nanoparticles.

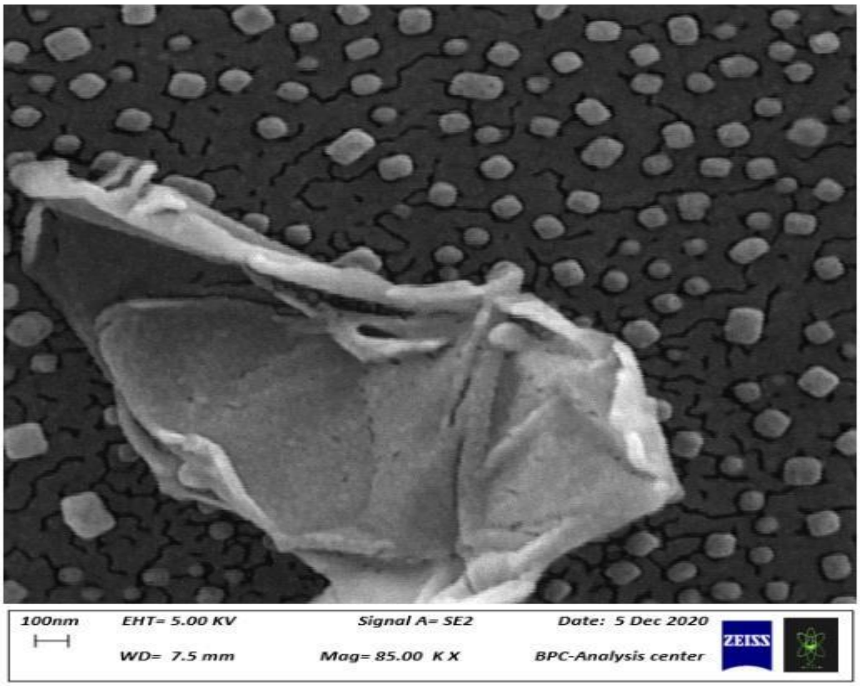

Fig 4.1 (G : Ag)

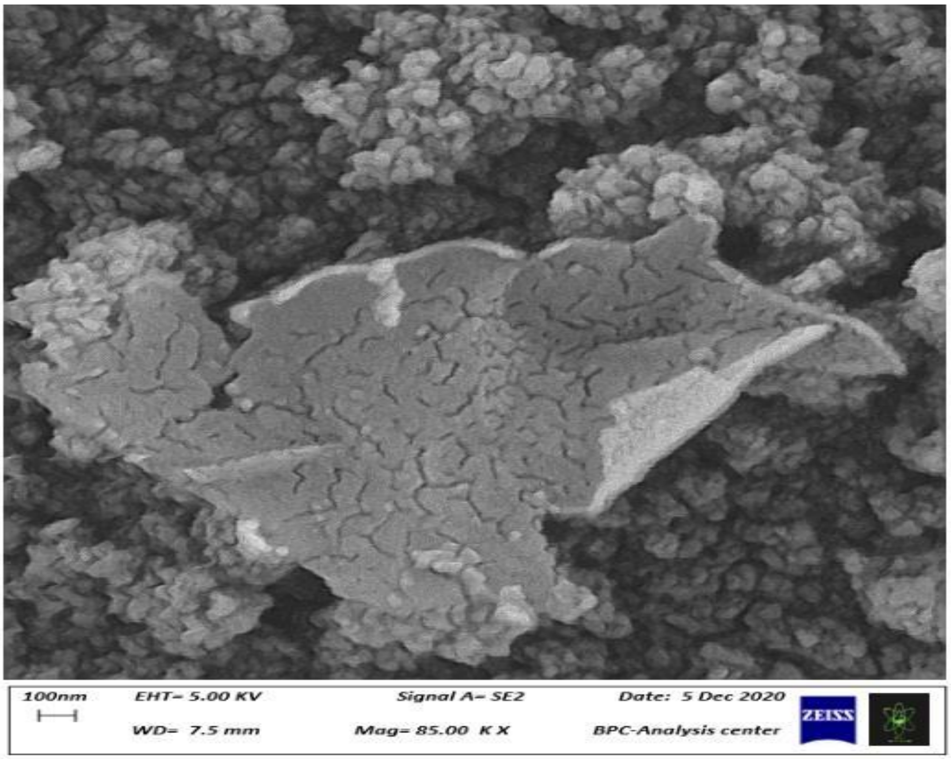

Fig 4.2 (G :TiO_2)

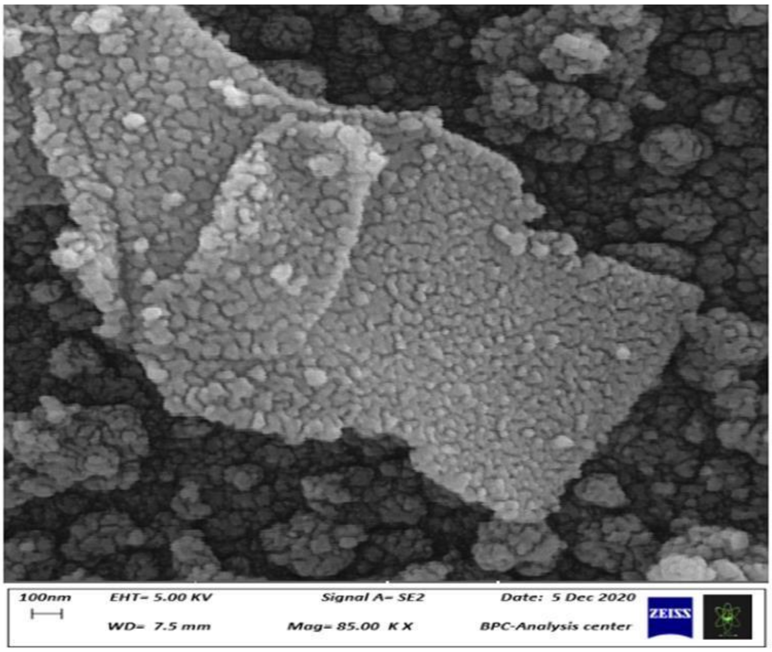

Fig 4.3 (G : Ag: TiO_2)

4.2 Oxygen detector

Type	Temperature ($T^{o}C$)	Sensitivity (S%)	Response time (t_s sec)	Recovery time (t_{rec} sec)
G+Ag	RT	6.34	58	13
	50	18.78	62	68
G+TiO2	RT	17.9	25	22
	50	18.7	17	3
G+TiO2+Ag	RT	64.6	35	90
	50	30.48	88	10

Table 4.1 shows the rati Sensitivity o at room temperature(RT) and $50^{o}C$

The first sample (G:Ag) at RT had a response of Sensitivity(6.34) as in shown Table (4.1) and as shown in the picture(4.4) .

But at $50^{o}C$ degrees, the response was Sensitivity (18.78) as in Table (4.1) and as shown in the Fig (4.5)

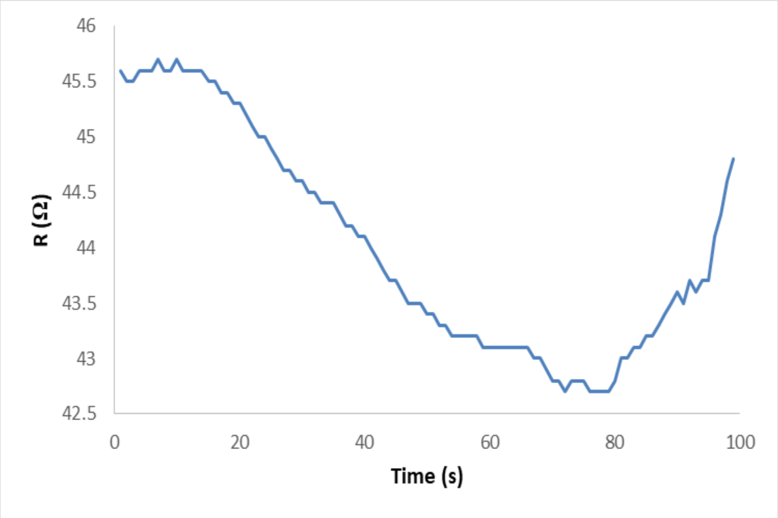

Fig 4.4 Resistance-time variation of G+Ag sensor at RT testing temperature

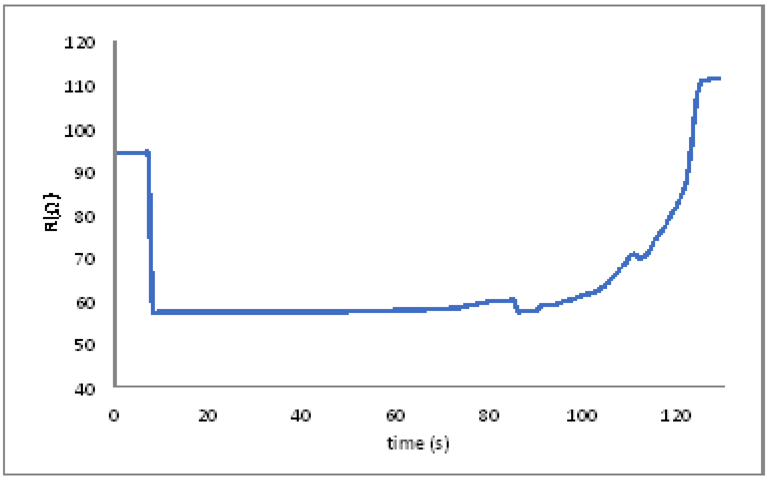

Fig 4.5 Resistance-time variation of G+Ag sensor at 50 ^{o}C testing temperature

The second sample (G:TiO2) at RT had a response of Sensitivity(17.9) as in shown Table (4.1) and as shown in the picture(4.6) .

But at 50^{o}C degrees, the response was Sensitivity (18.7) as shown in Table (4.1) and as shown in the Fig (4.5)

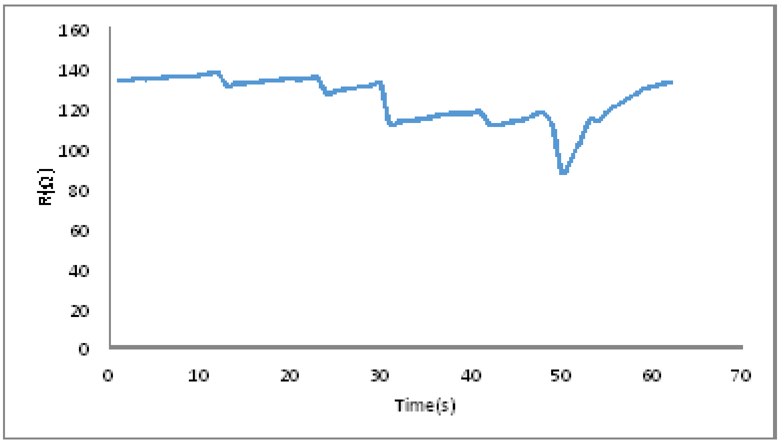

Fig 4.6 Resistance-time variation of TiO2 sensor at RT testing temperature

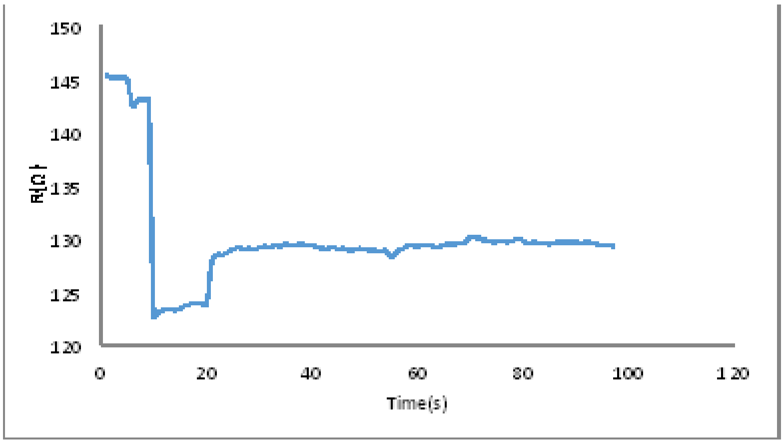

Fig 4.7 Resistance-time variation of TiO2 sensor at 50 ^{o}C testing temperature

The third sample (G:TiO2:Ag) at RT had a response of Sensitivity(64.6) as in shown Table (4.1) and as shown in the picture(4.8) .

But at 50^{o}C degrees, the response was Sensitivity (30.48) as in Table (4.1) and as shown in the

Fig (4.9).

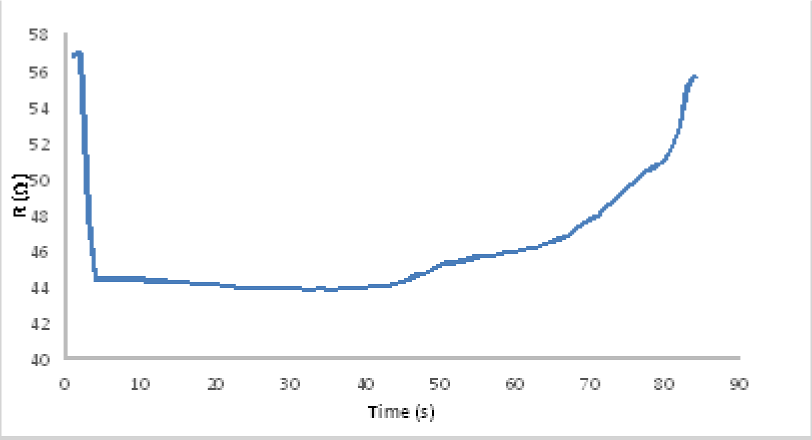

Fig 4.8 Resistance-time variation of G+TiO2+Ag sensor at RT testing temperature

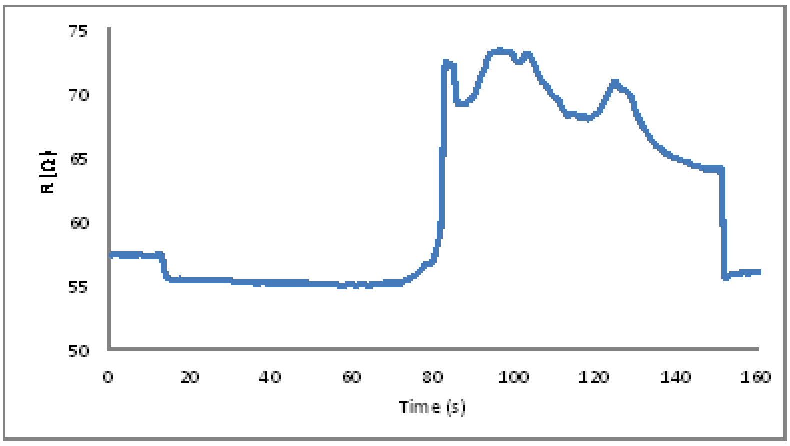

Fig 4.9 Resistance-time variation of G+TiO2+Ag sensor at 50 °C testing temperature.

5.1 conculsion

1. successful manufacturing the sensors of oxgen by use LIFT method.
2. high response of oxygen for G+Ag +TiO2 than G+Ag and G+ TiO2.

5.2 future work

1. detect another gas like H2S or NiO2 and CO2.
2. using silicon substrate as base of sensor.
3. replace the Ag nanoparticles by plant extraction.

Reference

1. P. Serra and A. Pique, “laser – induced forward transfer : Fundamentals and application”, *advanced material technology*, vol. 4 p:p 1-4, 2019.
2. M. Eslamian and F. Soltani-Kordshuli “ Development of multiple-droplet dropcasting method for the fabrication of coatings and thin solid films” *Journal of Coatings Technology and Research*, vol. 15, pp.271–280, 2018.
3. A. Piqué and H. Kim, “Laser-Induced Forward Transfer of Functional Materials: Advances and Future Directions”, *JLMN-Journal of Laser Micro/ Nano engineering*, Vol. 9, No. 3, 2014.

4. Z. Mucsi, G. A. Chass, P. Ábrányi-Balogh, B. Jójárt, D.-C. Fang, A. J. Ramirez-Cuesta, B. Viskolczc and I. G. Csizmadia, Phys. Chem. Chem. Phys., 2013, 15, 20447
5. K.K.H. De Silva , H.H. Huang , R.K. Joshi , M. Yoshimura, “chemical reduction of graphene oxide using green reductant”, *Elsevier Carbon*, vol. 119 p.p. 190 – 199, 2017.
6. M. Jia and Y. Tai, “green synthesis of reduced graphene oxide using green tea extra” *AIP Conference Proceedings*, vol.2045, pp. 1-7, 2017.
7. P. Sopeña, S. González-Torres,Juan M. F. Pradas, P. Serra, “Spraying dynamics in continuous wave laser printing of conductive inks”, *Chem. Rev*., vol. 107, pp. 2411250, 2017.
8. T. Araki, R. Mandamparambil, D. Martinus Peterus, J. Jiu, H. Koga, J. van den Brand, T. Sekitani, J. M J den Toonder and K. Suganuma, “Stretchable and transparent electrodes based on patterned silver nanowires by laser-induced forward transfer for non-contacted printing techniques” , *Nanotechnology*, Vol. 27, No. 45, 2016.
9. W. Huan, W. Yong, C. Xuemei, “Synthesis of uniform silver nanowires from AgCl seeds for transparent conductive films via spin-coating at variable spin-speed”, *Elsevier B.V*., vol. 565, no. 4 pp. 154- 161, 2019.
10. M. Praeger, S. Papazoglou, “Laser-induced backward transfer of monolayer graphene”, *Applied Surface Science*, vol. 533, p. 147488, 2020.
11. X. Wang, J. Zhang, X. Mei, J. Miao and X. Wang, “Laser-induced forward transfer of graphene oxide”, *Applied Physics A* vol. 127, no. 207, 2021.
12. T. Sano , H. Yamada , T. Nakayama , I. Miyamoto, “experimental investigation of laser induced forward transfer process of metal thin film”, *applied surface science*, vol. 186 p:p 221- 226, 2002
13. Ö. Cengiz, J.B. Hess, S.F. Bilgili :Influence of graded levels of dietary sodium on the development of footpad dermatitis in broiler chickens
14. X. Wang, J. Zhang, X. Mei, J. Miao and X. Wang, “Laser-induced forward transfer of graphene oxide”, Applied Physics A vol. 127, no. 207, 2021
15. T. Sano , H. Yamada , T. Nakayama , I. Miyamoto, “experimental investigation of laser induced forward transfer process of metal thin film”, applied surface science, vol. 186 p:p 221- 226, 2002.
16. Mallard LM, Pimenta MA, Dresselhaus G, Dresselhaus MS. Raman spectroscopy in graphene. Physics Reports. 2009;473:51-87
17. Geim AK, Kim P. Carbon wonderland. Scientific American. 2008;298:90
18. Novoselov KS, Geim AK, Morozov SV, Jiang D, Zhang Y, Dubonos SV, et al. Electric field effect in atomically thin carbon films. Science. 2004;306:666
19. Viculis LM, Mack JJ, Kaner RB. A chemical route to carbon nanoscrolls. Science. 2003;299:1361
20. Berger C, Song Z, Li T, Li X, Ogbazghi AY, Feng R, et al. Ultrathin epitaxial graphite: 2D electron gas properties and a route toward graphene-based nanoelectronics. The Journal of Physical Chemistry. 2004;108:19912
21. Land TA, Michely T, Behm RJ, Hemminger JC, Comsa G. STM investigation of single layer graphite structures produced on Pt(111) by hydrocarbon decomposition. Surface Science. 1992;264:261

22. Kumar, Challa Vijaya, and Ajith Pattammattel. Introduction to Graphene: Chemical and Biochemical Applications. Elsevier, 2017.

23. Chen, Long, et al. "ChemInform Abstract: From Nanographene and Graphene Nanoribbons to Graphene Sheets: Chemical Synthesis." ChemInform, vol. 44, no. 2, Aug. 2013, doi:10.1002/chin.201302190.

24. Guldi, Dirk M., and Nazario Martin. Carbon nanotubes and related structures synthesis, characterization, functionalization, and applications. Weinheim, WileyVCH, 2010.

25. Pisula, Wojciech, et al. "Charge-Carrier Transporting Graphene-Type Molecules†." Chemistry of Materials, vol. 23, no. 3, Aug. 2011, pp. 554–567., doi:10.1021/cm102252w.

26. Warner, Jamie H., et al. Graphene: Fundamentals to emergent applications. Kidlington, Oxford, Elsevier, 2013.

27. Sharma, Kal R. Graphene nanomaterials. New York, Momentum Press, 2014.

28. Nazarpour, Soroush, and Stephen R Waite. *Graphene technology: From Laboratory to Fabrication*. Weinheim, Wiley Vch Publication, 2016.

29. Sood, Ashok K., et al. "Review of Graphene Technology and Its Applications for Electronic Devices." *Review of Graphene Technology and Its Applications for Electronic Devices | InTechOpen*, InTech, 25 Nov. 2015. Accessed 20 Sept. 2017.

30. Fujishima, A.; Honda, K. Nature 1972, 238, 37.

31. Linsebigler, A. L.; Lu, G.; Yates, J. T. Chem. Rev. 1995, 95, 735

32. Hoffmann, M. R.; Martin, S. T.; Choi, W.; Bahnemann, D. W. Chem. Rev. 1995, 95, 69

33. Thompson, T. L.; Yates, J. T., Jr. Chem. Rev. 2006, 106, 4428

34. Chen, X.; Mao, S. S. Chem. Rev. 2007, 107, 2891

35. Chen, H.; Nanayakkara, C. E.; Grassian, V. H. Chem. Rev. 2012, 112, 5919

36. Zhang, Z.; Yates, J. T., Jr. Chem. Rev. 2012, 112, 5520

37. Henderson, M. A.; Lyubinetsky, I. Chem. Rev. 2013, 113, 4428

38. Pang, C. L.; Lindsay, R.; Thornton, G. Chem. Rev. 2013, 113, 3887

39. Sang, L.; Zhao, Y.; Burda, C. Chem. Rev. 2014,

40. Cargnello, M.; Gordon, T. R.; Murray, C. B. Chem. Rev. 2014,

41. Wang, X.; Li, Z.; Shi, J.; Yu, Y. Chem. Rev. 2014,

42. Lee, K.; Mazare, A.; Schmuki, P. Chem. Rev. 2014,

43. Wang, L.; Sasaki, T. Chem. Rev. 2014,

44. Fattakhova-Rohlfing, D.; Zaleska, A.; Bein, T. Chem. Rev. 2014,

45. Liu, G.; Yang, H. G.; Pan, J.; Yang, Y. Q.; Lu, G. Q. (Max); Cheng, H.- M. Chem. Rev. 2014,

46. Zhang, H.; Banfield, J. F. Chem. Rev. 2014,

47. Coppens, P.; Chen, Y.; Trzop, E. Chem. Rev. 2014,

48. Kapilashrami, M.; Zhang, Y.; Liu, Y.-S.; Hagfeldt, A.; Guo, J. Chem. Rev. 2014,

49. De Angelis, F.; Di Valentin, C.; Fantacci, S.; Vittadini, A.; Selloni, A. Chem. Rev. 2014,

50. Bourikas, K.; Kordulis, C.; Lycourghiotis, A. Chem. Rev. 2014,
51. Asahi, R.; Morikawa, T.; Irie, H.; Ohwaki, T. Chem. Rev. 2014,
52. Dahl, M.; Liu, Y.; Yin, Y. Chem. Rev. 2014,
53. Liu, L.; Chen, X. Chem. Rev. 2014,
54. Schneider, J.; Matsuoka, M.; Takeuchi, M.; Zhang, J.; Horiuchi, Y.; Anpo,
55. M.; Bahnemann, D. W. Chem. Rev. 2014, dx.doi.org/10.1021/cr5001892
56. Ma, Y.; Wang, X.; Jia, Y.; Chen, X.; Han, H.; Li, C. Chem.
57. Rev. 2014, dx.doi.org/10.1021/cr500008u
58. Liu, K.; Cao, M.; Fujishima, A.; Jiang, L. Chem.
59. Rev. 2014, dx.doi.org/10.1021/cr4006796
60. Bai, Y.; Mora-Seró, I.; De Angelis, F.; Bisquert, J.; Wang, P. Chem. Rev. 2014, dx.doi.org/10.1021/cr400606n
61. Bai, J.; Zhou, B. Chem. Rev. 2014, dx.doi.org/10.1021/cr400625j
62. Rajh, T.; Dimitrijevic, N. M.; Bissonnette, M.; Koritarov, T.; Konda, V. Chem.
63. Rev. 2014, dx.doi.org/10.1021/cr500029g

    (Mafune et al. 2000; Mafune et al. 2001; Kabashin and Meunier 2003; Sylvestre et al. 2004; Dolgaev et al. 2002).

64. Senapati 2005; Klaus-Joerger et al. 2001

    (Kim et al. 2005; Link et al. 2000; Tarasenko et al. 2006; Kawasaki and Nishimura 2006)

    This Article was written by M.Keerthana,Biomedical Engineer,Customer Care Specialist

65. Russo, P. A. et al. Room-temperature hydrogen sensing with hetero nanostructures based on reduced graphene oxide and tin oxide. Angew. Chemie - Int. Ed. 51, (11053–11057 (2012).
66. Segev-Bar, M. & Haick, H. Flexible sensors based on nanoparticles. ACS Nano 7, 8366–8378 (2013).
67. Martins, P., Lopes, A. C. & Lanceros-Mendez, S. Electroactive phases of poly(vinylidene fuoride): Determination, processing and applications. Prog. Polym. Sci. 39, 683–706 (2014).
68. Cauda, V., Stassi, S., Bejtka, K. & Canavese, G. Nanoconfnement: An efective way to enhance PVDF piezoelectric properties. ACS Appl. Mater. Interfaces 5, 6430–6437 (2013).
69. Punetha, D. & Pandey, S. K. CO Gas Sensor Based on E-Beam Evaporated ZnO, MgZnO, and CdZnO Tin Films: A Comparative Study. IEEE Sens. J. 19, 2450–2457 (2019).
70. Kaniyoor, A., Imran Jafri, R., Arockiadoss, T. & Ramaprabhu, S. Nanostructured Pt decorated graphene and multi walled carbon nanotube based room temperature hydrogen gas sensor. Nanoscale 1, 382–386 (2009).
71. Virji, S., Kaner, R. B. & Weiller, B. H. Hydrogen sensors based on conductivity changes in polyaniline nanofbers. J. Phys. Chem. B 110, 22266–22270 (2006).
72. Peng, Y., Ye, J., Zheng, L. & Zou, K. Te hydrogen sensing properties of PtPd/reduced graphene oxide based sensor under diferent operating conditions. RSC Adv. 6, 24880–24888 (2016).
73. Dubinin, M. M. Te potential theory of adsorption of gases and vapors for adsorbents with energetically nonuniform surfaces. Chem. Rev. 60, 235–241 (1960).

74. Kumar, R. et al Fast response and recovery of hydrogen sensing in Pd-Pt nanoparticle-graphene composite layers. Nanotechnology 22 (2011).
75. Punetha, D., Dixit, H. & Pandey, S. K. Modeling and analysis of an Ni:ZnObased Schottky pattern for NO2 detection. J. Comput. Electron. 18, 300–307 (2019).
76. Mokrushin, Artem S.; Fisenko, Nikita A.; Gorobtsov, Philipp Yu. "Pen plotter printing of ITO thin film as a highly CO sensitive component of a resistive gas sensor". Talanta. 221: 121455. doi:10.1016/j.talanta.2020.121455.
77. Detcon, www.detcon.com/electrochemical01.htm Archived 2009-05-05 at the Wayback Machine
78. United States Patent 4141800: Electrochemical gas detector and method of using same, http://www.freepatentsonline.com/4141800.html
79. Jump up to:[a b c] Muda, R., 2009
80. International Society of Automation, http://www.isa.org/Template.cfm?Section=Communities&template=/TaggedPage/DetailDisplay.cfm&ContentID=23377 Archived 2013-12-12 at the Wayback Machine
81. *Naranjo, Edward (2010). Dinwiddie, Ralph B; Safai, Morteza (eds.). "IR gas imaging in an industrial setting". Thermosense XXXII. 7661: 76610K. doi:10.1117/12.850137. S2CID 119488975.*
82. Figaro Sensor, http://www.figarosensor.com/products/general.pdf
83. Jump up to:[a b] Vitz, E., 1995
84. General

    Monitors, http://www.generalmonitors.com/downloads/literature/combustible/IR2100_DATA.PDF
85. *Ghosh, Sujoy; Ilango, Murugaiya; Prajapati, Chandra; Bhat, Navakanta (7*
86. *January 2021). "Reduction of Humidity Effect in WO3 Thin Film-Based NO2 Sensor Using Physiochemical Optimization". Crystal Research & Technology. 56 (1): 2000155. doi:10.1002/crat.202000155. ISSN 1521-4079.*
87. *Ghosh, Sujoy; Ghosh, Anujay; Kodavali, Nived; Prajapati, Chandra Shekhar; Bhat, Navakanta (13 January 2020). A baseline correction model for humidity and temperature compensation WO3 film based sensor for NO2 detection. 2019 IEEE Sensors. Montreal, Canada: IEEE. doi:10.1109/SENSORS43011.2019.8956920. ISSN 2168-9229.*
88. Jumpto:[a b] Naranjo,

    E., http://www.gmigasandflame.com/article_october2007.html
89. *Martínez-Hurtado, JL; Davidson, CA; Blyth, J; Lowe, CR (2010). "Holographic detection of hydrocarbon gases and other volatile organic compounds". Langmuir. 26 (15694– doi:10.1021/la102693m. PMID 20836549.*